Atomic mechanism of internal friction in a model metallic glass

Hai-Bin Yu and Konrad Samwer
I. Physikalisches Institut, Universität Göttingen, D-37077 Göttingen, Germany
(Received 14 April 2014; revised manuscript received 16 September 2014; published 6 October 2014)

Internal friction (IF) describes the ability of materials to damp out mechanical oscillations. It is a crucial engineering parameter and also conveys unique microscopic information about structural defects, transport phenomena, and phase transformations in solids. While IF predominately results from lattice defects in crystalline materials, the origin of IF remains unclear in disordered materials, like metallic glasses. In this paper, we study the atomic rearrangements that govern IF in a model metallic glass, via numerical simulations of dynamical mechanical spectroscopy together with structural analysis. We identify cooperative and avalanchelike thermal-driven excitations as an underlying mechanism and demonstrate a linearlike relation between the concentrations of these excitations and the values of IF. Structurally, these excitations can be hindered, and thus suppress IF, by slow atoms that usually associate with full icosahedral symmetry. Our results also provide practical guides in tuning IF in metallic glasses from atomistic perspectives.

DOI: 10.1103/PhysRevB.90.144201 PACS number(s): 62.40.+i, 64.70.pe, 61.43.Bn

I. INTRODUCTION

Internal friction (IF) characterizes the energy dissipations during cyclic mechanical loading [[1–5]. It is responsible for the damping properties of materials and is the major concern in many engineering applications [1–7], ranging from shock absorbers and vibration and noise reduction in construction, automobiles, and aircraft (where high IF is required), to high-quality resonance devices and high-precision instruments and sensors (where low IF is required). Internal friction is also highly sensitive to the microstructures of materials [1–5,8]. It provides unique information about structural defects, transport phenomena, and phase transformations in solids. Internal friction forms the core of mechanical spectroscopy methods [1–4], which are widely used in solid state physics, physical metallurgy, and materials sciences [1–10].

While IF predominately results from lattice defects (e.g., interstitial atoms, dislocations, and grain boundaries) in crystalline solids [1–5,8,11], the origin of IF in glassy materials is still not clear [1–4]. Due to the disordered structures and the diverse relaxation dynamics of glasses [12,13], there are at least three basic questions still unaddressed: (i) Does IF in a glass involve all the atoms or just small fractions? (ii) What are the atomic rearrangements that govern IF in glasses? (iii) What kinds of atomic structures can give rise to high or low values of IF for a specific application purpose?

Metallic glasses (MGs) [14,15], combining metallic bonding and disordered atomic structures [16,17], have received attention as ideal systems for studying fundamental issues in materials sciences [18,19]. Especially, taking advantage of their relatively simple atomic structures, which are amenable to modeling and analysis, molecular dynamics (MD) simulations have been utilized to investigate the intrinsic connections between the atomic structures and properties of MGs [17]. High-quality interatomic potentials, which are the essential inputs of MD simulations, are available for realistic computations [17]. In this paper, we use MD simulations to address the aforementioned basic questions and to explore the atomic mechanism of IF in MGs. Besides its fundamental significance, we note that clarification of IF in MGs is of practical importance. For example, some MGs have very low IF (thus, a high-quality factor) and high elasticity at room temperature, and they are now candidate materials for applications in, e.g., sports and microelectromechanical systems. On the other hand, some MGs with high IF related to secondary relaxations at relatively low temperatures could exhibit good ductility and are favored for damage-tolerant applications [18,19]. Internal friction and the related mechanical spectra contain important information about the relaxation dynamics, which are the central themes of glassy physics [18,19]. Internal friction could also relate to the glass-forming ability of MGs [19], which is a key issue in the fabrication of MGs. We note that although IF in MGs has been experimentally studied for several decades [20–27], a clear picture of its underlying mechanism is still lacking.

II. MODEL AND METHODS

A. Model systems

To characterize IF, in this paper we introduce a methodology for molecular dynamics simulation of dynamical mechanical spectroscopy (MD-DMS), which is based on real DMS experiments [18,19] and a recent simulation [28]. Two systems, with different cell sizes, were calculated independently. A larger system contains $N = 32\,000$ atoms, while a smaller system contains $N = 4000$ atoms. Both systems have the same composition $Cu_{65}Zr_{35}$, and the constituting atoms are interacted with an embedded atom method (EAM) potential [29]. For the sample preparations, both systems were melted and equilibrated at $T = 3000$ K and then cooled down to $T = 100$ K with a cooling rate of 10^{12} K/s, during which the cell sizes were adjusted to give zero pressure with the constant number, pressure and temperature (*NPT*) ensemble. Periodic boundary conditions were applied for all the calculations.

B. Molecular dynamics simulation of dynamical mechanical spectroscopy

Like real DMS [18,19], we apply a sinusoidal strain $\varepsilon(t) = \varepsilon_A \sin(2\pi t/T_\omega)$ along the x direction of the model MG, where T_ω is the period and is selected as 10, 30, 100, 300, and 1000 ps in this paper. We fix $\varepsilon_A = 2.5\%$, which is in the

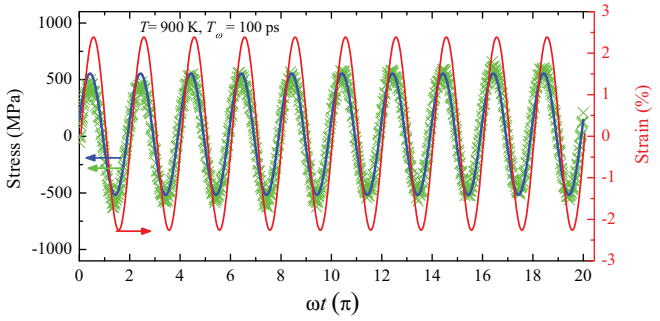

FIG. 1. (Color online) Typical MD-DMS curves at $T = 900$ K, $T_\omega = 100$ ps. (red, right axis) The applied sinusoidal strain. (green, left axis) The resultant stress that is fitted by a sinusoidal function (blue, left axis).

apparent linear elastic regime. (Note the yield strain is about 5% for the simulations.) For each MD-DMS, 10 full cycles were used, i.e., t in the range $[0, 10T_\omega]$. We fitted the resultant stress as $\sigma(t) = \sigma_0 + \sigma_A \sin(2\pi t/T_\omega + \delta)$, where σ_0 is a linear term and usually small, and δ is the phase difference between stress and strain. Storage (E') and loss (E'') modulus values are calculated as $E' = \sigma_A/\varepsilon_A \cos(\delta)$ and $E'' = \sigma_A/\varepsilon_A \sin(\delta)$, respectively. Figure 1 shows a typical MD-DMS measurement at $T = 900$ K with $T_\omega = 100$ ps.

In this paper, we prefer to use δ directly as a measure of IF, rather than $\tan(\delta)$, although $\tan(\delta)$ is commonly used in experiments. This is because at small values, $\delta \approx \tan(\delta)$, while

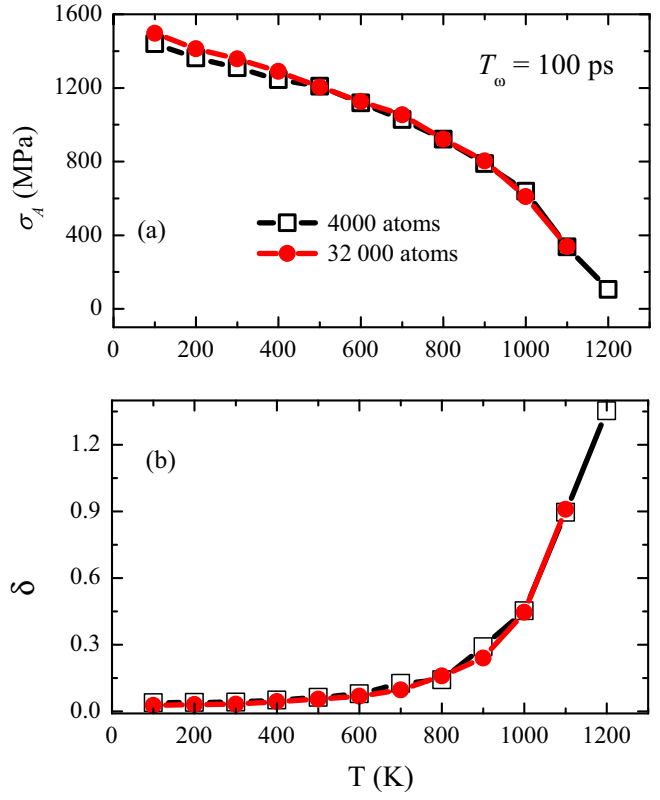

FIG. 2. (Color online) System size effects of the results of MD-DMS. The results from different system size (number of atoms) for (a) the stress amplitudes and (b) the phase angle.

at larger values as $\delta \to \pi/2$, $\tan(\delta)$ approaches ∞ and could result in significant and unphysical error bars, whereas the error bars for δ are still small. The MD-DMS was carried out during the cooling processes of the sample preparations, and the constant number, volume and temperature (*NVT*) ensemble was applied during the cyclic deformations. We have verified that the larger ($N = 32\,000$) and the smaller ($N = 4000$) systems give the same results, as shown in Fig. 2. Note, unless mentioned explicitly, all the results presented in this paper were from the larger system with $N = 32\,000$ atoms.

III. MECHANISM OF IF AS REVEALED BY MD-DMS AND STRUCTURAL ANALYSIS

A. Studying IF by MD-DMS

The stress amplitude σ_A and the phase angle δ between stress and strain are recorded as functions of temperature T for different periods T_ω (related to the frequency $f = 1/T_\omega$) and are reported in Fig. 3(a) and Fig. 3(b), respectively. From these two quantities, we derive the storage modulus E', and the loss modulus E'', as shown in Fig. 3(c) and Fig. 3(d), respectively. At low temperatures ($T < 600$ K), both E' and E'' change slightly with T. Then, at higher T, one can observe the sudden drops of E' as well as the asymmetrical peaks of E'' corresponding to α relaxations, signaling the transition from glassy to supercooled liquid states. These features are consistent with experimental DMS findings (e.g., Refs. [18,19]). Figure 4(a) plots the T_ω dependent peak temperature of E'' (which is the α relaxation temperature T_α at the corresponding α relaxation time $\tau_\alpha = T_\omega$). For comparison, we calculated τ_α (T) by the decay of the self-part of the intermediate scattering function (ISF), which is the most commonly used method in simulations of glassy dynamics, as shown in Fig. 4(b). The τ_α is determined when ISF decays to e^{-1} (the dashed horizontal line) for a given T. One can see that these two data sets from MD-DMS and ISF follow the same trend, which can be fitted by a unique Vogel-Fulcher-Tammann (VFT) equation [13], $\tau_\alpha = \tau_0 \exp B/(T - T_0)$, where τ_0, B, and T_0 are parameters. This confirms the validity and reliability of our MD-DMS in studying the relaxation dynamics of glasses.

We then focus on the values of δ [Fig. 3(b)], which characterize IF of the model MG. The following salient features can be summarized: (i) In the temperature range below 600 K, IF at any T_ω is low ($\delta \leqslant 0.1$) and its temperature dependence is weak. (ii) Above $\sim 0.7\ T_\alpha$, a stronger T and T_ω dependence and a much more rapid increase of IF set in and continue, suggesting that structural arrangements related to IF occur and persist. (iii) At any temperature, IF is frequency dependent, and the values of δ are greater at larger T_ω (or lower f). We note all these features are also qualitatively consistent with experimental observations of IF in MGs [18–27]. These agreements demonstrate again the robustness of MD-DMS for studying IF in MGs.

B. Atomic rearrangements governing IF

To explore the underlying atomic rearrangements that govern IF in MGs, we utilize the ability of MD simulations to examine individual atomic jump processes. We calculate the mean square atomic jump distance u for each atom during a time interval of $\Delta t = T_\omega$ for every combination of T and T_ω.

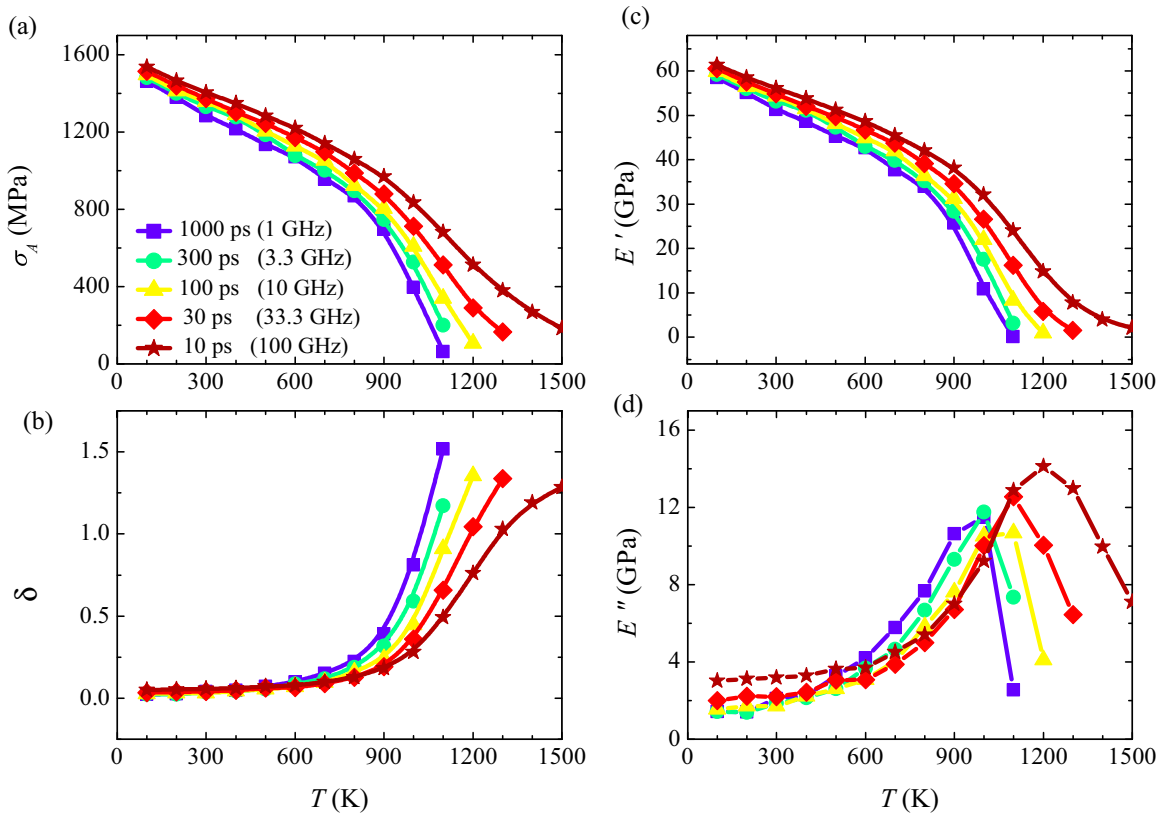

FIG. 3. (Color online) (a) Stress amplitude σ_A, (b) phase angle δ, (c) storage modulus E', and (d) loss modulus E'', as functions of temperature T, for different T_ω or f in the parentheses as indicated in (a).

Such a selection of Δt is to avoid atomic displacements due to the overall deformations applied by the MD-DMS. Figure 5(a) shows a typical set of the resultant distribution density functions $p(u)$ at $T = 900$ K (in glassy state) for different values of T_ω. One can see that these curves overlap around a peak with $u_p \approx 0.35$ Å, which represents the most probable value of u of all the atoms. On the other hand, remarkable differences can be discerned on the tails of $p(u)$: the larger the value of T_ω, the higher $p(u)$ reaches and the farther u extends. Comparing $p(u)$ with the results of IF shown in Fig. 3(b), we note the tails, rather than the peaks, of $p(u)$ evolve with the same T_ω dependence as IF at a given T. This implies IF could be related to the rearrangements of only a small fraction of atoms with u larger than u_p. Figure 3(b) shows u_p as a function

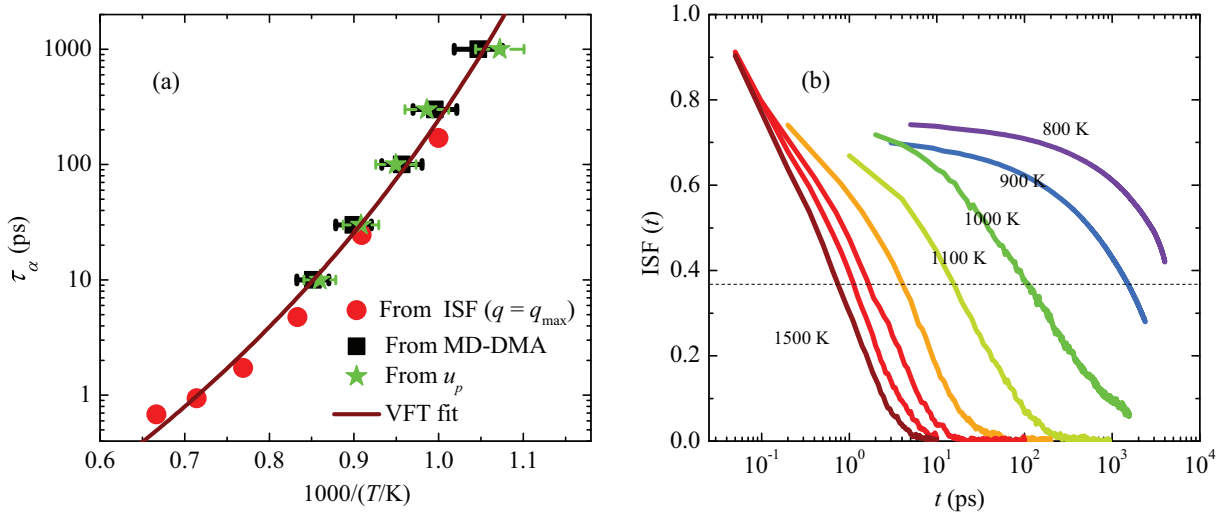

FIG. 4. (Color online) (a) The T dependent α relaxation time $\tau_\alpha(T)$. Three data sets are calculated by different methods as indicated, and they are fitted by a VFT function. (b) ISF of the model MG at temperatures between 800 and 1500 K at every 100 K. The τ_α is determined when ISF decays to e^{-1} (the dashed horizontal line) for a given T.

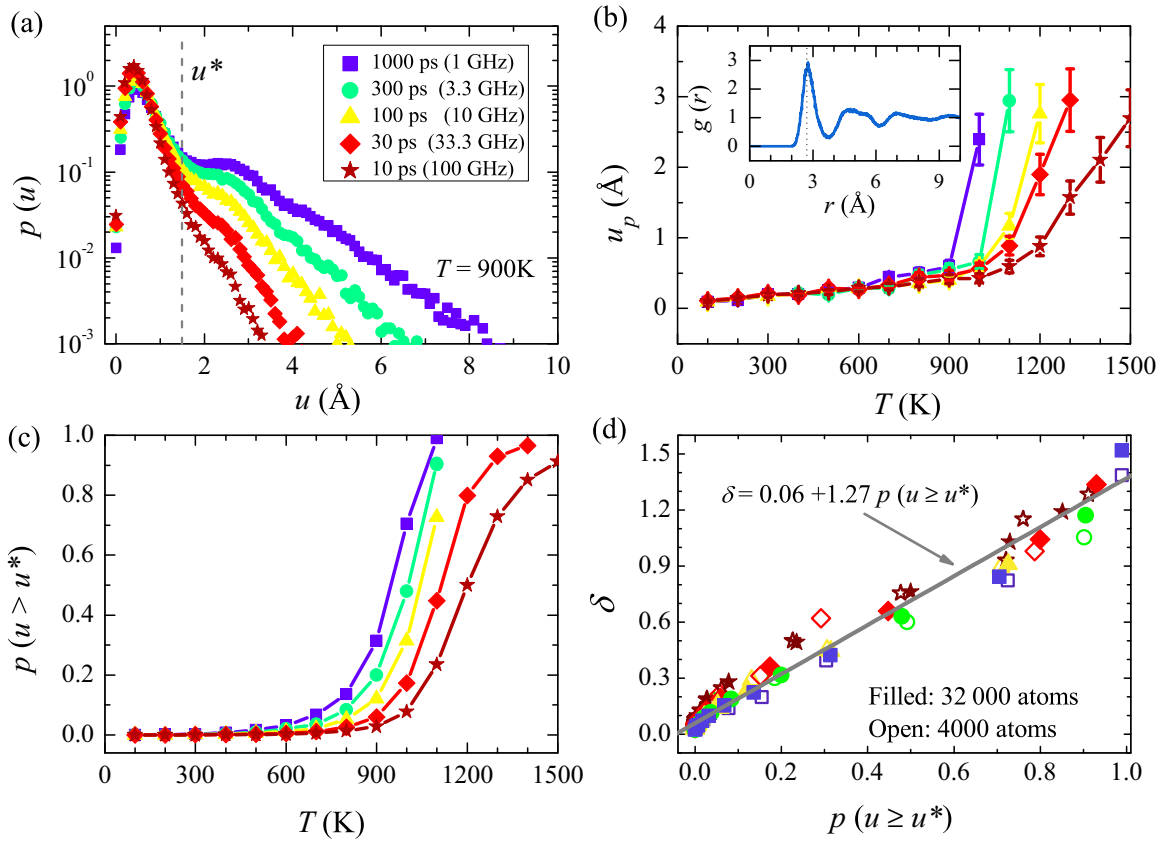

FIG. 5. (Color online) Structural analysis based on the mean square atomic jump distance u. (a) Statistical distribution $p(u)$, at $T = 900$ K, for different T_ω or f in the parentheses. (b) The T dependence of the peak position u_p of $p(u)$ for different T_ω. The inset of (b) is $g(r)$ at $T = 900$ K. (c) The T dependence of the distribution $p(u > u^*)$ with $u^* = 1.4$ Å. (d) Relationship between δ and $p(u > u^*)$; the line is a least-square fit. The symbols in (b), (c), and (d) have the same meanings as those in (a).

of T and T_ω; one can see that u_p is nearly independent of T_ω in the glassy state, while appreciable T_ω dependence of u_p sets in for the supercooled liquid states. [Note the temperature at which the slope of u_p (T) changes is T_α, as shown in Fig. 4.] This fact, in contrast with the T_ω dependence of IF [Fig. 3(b)] in *both* the glassy and supercooled liquid states, confirms that IF is not due to the rearrangements of all the atoms globally.

To better reveal the atomic motions that govern IF in the model MG, we define the group of "faster atoms"; i.e., those atoms with u larger than a critical value, u^*. According to a cooperative shear model (CSM) [30,31], we take $u* = r_0/2 = 1.4$ Å, where $r_0 \approx 2.8$ Å is the average nearest neighbor distance, which is determined from the radial distribution function $g(r)$ as shown in the inset of Fig. 5(b). In CSM [30,31], u^* is the minimum distance that an atom must move to enable it to jump from one stable configuration to another. Figure 5(c) depicts the fractions of "faster atoms" $p(u \geqslant u^*)$ as a function of T for different T_ω. We note that $p(u \geqslant u^*)$ in Fig. 5(c) and the values of δ in Fig. 3(b) have the nearly the same T and T_ω dependence, suggesting "faster atoms" could be an underlying mechanism of IF. To check this conjecture, we plot the values of δ against $p(u \geqslant u^*)$ in Fig. 5(d). Surprisingly, the data reveal nearly a one-to-one correspondence between δ and $p(u \geqslant u^*)$ for all the combinations of T and T_ω, and extend over a broad range. We find a linearlike relationship between these two quantities: $\delta \approx 0.06 + 1.27 p(u \geqslant u^*)$. At the same time, we notice the scattering of the data is reduced for larger systems in our simulations. For instance, the least-square linear fit gives a correlation coefficient $R^2 \approx 0.92$ for the smaller system with the number of atoms $N = 4000$, while $R^2 \approx 0.95$ for the larger system with $N = 32\,000$, although periodic boundary conditions are applied for both systems. This system size dependence implies that the correlation between δ and $p(u \geqslant u^*)$ should hold much better for macroscopic systems with $N \sim 10^{23}$. So far, we have established a correlation between IF and concentrations of "faster atoms" that can escape from one stable configuration during a given time interval T_ω at T. This result, representing one of the major findings of this paper, is also reminiscent of the general view in crystalline materials that defects determine the IF of materials [1–4].

We next study the spatial distributions of these "faster atoms". Figure 6(a) shows the atomic configurations on a slice of the xy plane (with $20 < z \leqslant 24$, $T = 900$ K, $T_\omega = 100$ ps or $f = 10$ GHz) with the color code on each atom representing the magnitude of the u value. One can see that these atoms with larger u values are heterogeneously distributed and have a strong tendency to aggregate and to form clusterlike structures, suggesting these "faster atoms" could be a kind of cooperative excitation. This observation is consistent with the physical picture of the dynamical heterogeneity of glasses and supercooled liquids [32–34]. Figure 6(b) presents

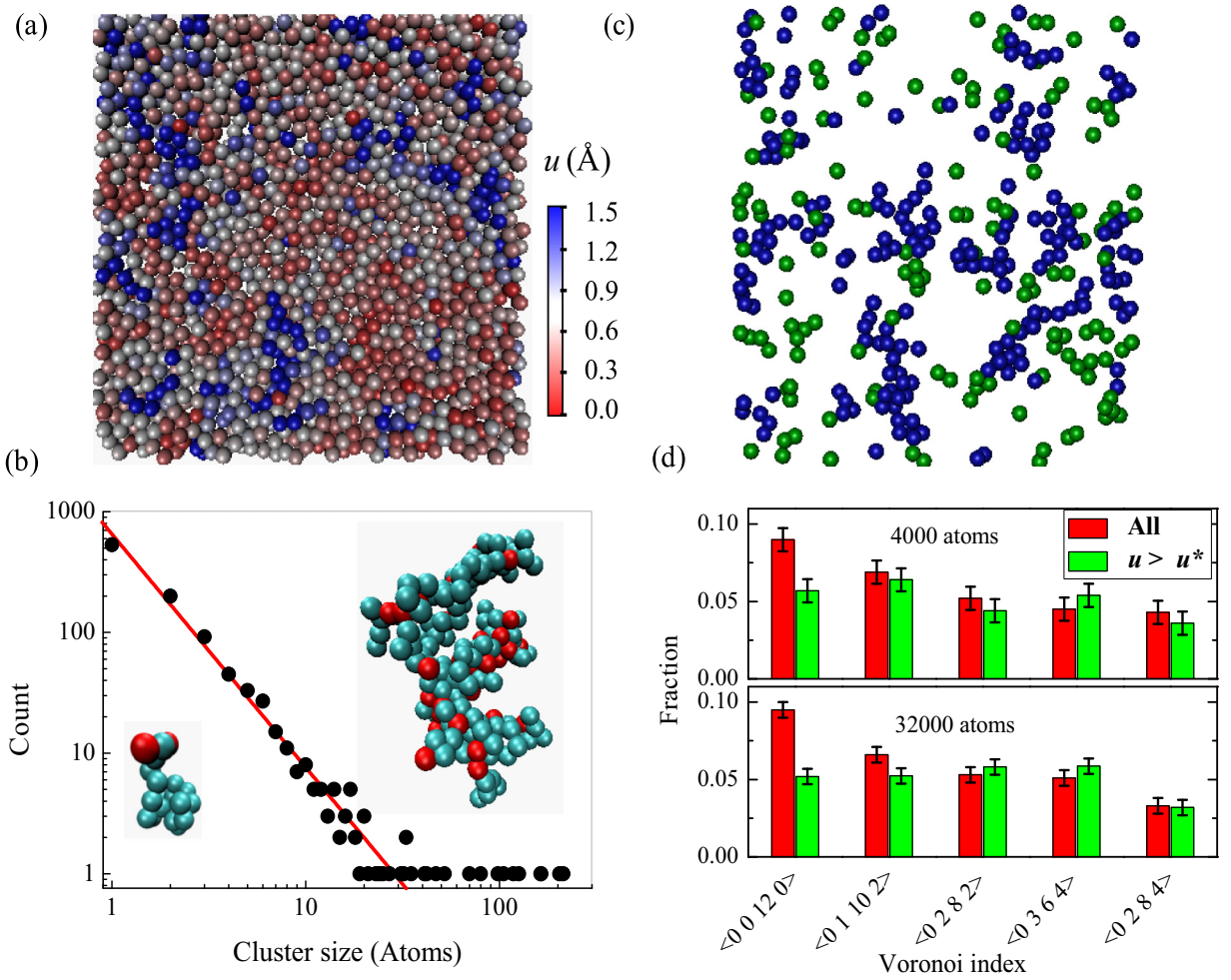

FIG. 6. (Color online) Spatial distributions and structural features of "faster atoms". (a) A 2D slice of the atomic configuration at $T = 900$ K, $T_\omega = 100$ ps (or $f = 10$ GHz), with color code on each atom representing the value of u. (b) Discrete count of the number of atoms in the clusters with $u \geqslant u^*$. The inset of (b) shows two such typical clusters, where the red balls represent Cu atoms, while the green balls represent Zr atoms. (c) Spatial distribution of "faster atoms" (blue) with $u > u^*$ and atoms with icosahedral symmetry (green). (d) Statistical histogram of the fractions of atoms with different Voronoi indexes for all the atoms and for atoms with $u > u^*$.

a discrete count of the number of atoms in these clusterlike excitations with $u \geqslant u^*$ ("faster atoms" as defined above) at $T = 900$ K and $T_\omega = 100$ ps. We find the typical sizes of clusters range from 1 to about 200 atoms and are distributed following a power law with an exponent about -1.6 ± 0.2 for the small to intermediate size clusters and a tail for very large clusters. Such a power law distribution is similar to the avalanche behaviors as found in many different systems [35–37], and a critical point is reached when one supercluster spans all the "faster atoms" (percolation). A closer examination of the atomic trajectories also suggests that these excitations are avalanchelike: Atoms with $u \geqslant u^*$ can trigger their neighbors in an intermittent stochastic fashion. Overall, we learn that the "faster atoms" (that govern IF of the model MG) are cooperative thermal-driven excitations with avalanchelike behaviors.

C. Relating IF to atomic structures

To ultimately relate these thermal excitations that govern the IF of the model MG with atomic structures, we analyze the atomic coordinates with a Voronoi tessellation method, which divides space into close-packed polyhedra around atoms by construction of bisecting planes along the lines joining the central atom and its neighbors [17]. In such a way, each atom is associated with a Voronoi index $\langle n_3 n_4 n_5 n_6 \rangle$, with n_i denoting the number of i-edged faces of its polyhedron. Especially, it has been known that atoms with full icosahedral symmetry ($\langle 0\ 0\ 12\ 0 \rangle$) play important roles in the formation, mechanical properties, and relaxation dynamics of glasses [[17,38–42]. Such atoms are in the center of the icosahedral polyhedra, with fivefold symmetry for each face (pentagons). Figure 6(c) shows a snapshot of the atoms with full icosahedral symmetry (green color) together with the "faster atoms" (blue color). We find, statistically, these two species of atoms tend to avoid each other: There are very few atoms with full icosahedral symmetry in the regions of "faster atoms", and vice versa. This suggests "faster atoms" and atoms with full icosahedral symmetry are anticorrelated. Figure 6(d) compares the fractions of the major Voronoi indexes for the whole system and for those "faster atoms". We see again the "faster atoms" are associated less icosahedral polyhedra, corroborating faster atoms and icosahedra clusters are anticorrelated. On the other hand, our Voronoi analysis did not show certain types of clusters would

dominate "faster atoms"; instead, we find "faster atoms" are associated with a wide variety of low-population polyhedra with complex geometries.

IV. DISCUSSIONS AND SUMMARY

Our MD-DMS and structural analysis can be readily compared with experiments and have implications in controlling IF in MGs. For example, the atoms with full icosahedral symmetry in our model $Cu_{65}Zr_{35}$ MG are predominately centered on Cu. This implies that if Cu is replaced with other (chemically similar) atoms like Ni, IF could increase, which is indeed confirmed experimentally [43]. In addition, our previous experimental results have shown that alloying 1–4% Al into CuZr MGs can dramatically suppress the E'' and IF [43], while MD simulations indicate Al-alloying can increase the atoms with full icosahedral symmetry [17]; both are in good agreement with present findings. Therefore, our results provide not only insights into the mechanisms of IF in disordered materials, but also a practical guide in designing MGs with tunable IF from the atomic levels.

In summary, by introducing a MD-DMS methodology, we find IF in a model MG is governed by the fractions of atoms that jump faster than the most probable value. Spatially, these atoms are a kind of cooperative and avalanchelike thermal-driven excitation. Structurally, these excitations can be hindered by atoms with full icosahedral symmetry, thus suppressing IF. These excitations can be considered as transient defects in MGs. Our results also provide a practical guide in designing MGs with tunable IF from the atomic levels.

ACKNOWLEDGMENTS

The authors acknowledge the computational service from Gesellschaft für Wissenschaftliche Datenverarbeitung, Göttingen (GWDG), and financial support from the Deutsche Forschungsgemeinschaft (DFG) within the research unit FOR 1394.

[1] M. S. Blanter, I. S. Golovin, H. Neuhäuser, and H. R. Sinning, *Internal Friction in Metallic Materials: A Handbook* (Springer-Verlag, Berlin Heidelberg, 2007).
[2] C. M. Zener, *Elasticity and Anelasticity of Metals* (University of Chicago Press, Chicago, 1948).
[3] R. de Batist, *Internal Friction of Structural Defects in Crystalline Solids.* (North-Holland Publishing Company, Amsterdam, 1973).
[4] H. Wagner, D. Bedorf, S. Kuchemann, M. Schwabe, B. Zhang, W. Arnold, and K. Samwer, Nat. Mater. **10**, 439 (2011).
[5] J. Zhang, R. J. Perez, C. R. Wong, and E. J. Lavernia, Mater. Sci. Eng. R **13**, 325 (1994).
[6] W. Weaver, Jr., S. P. Timoshenko, and D. H. Young, *Vibration Problems in Engineering* (John Wiley & Sons, New York, 1990).
[7] M. D. LaHaye, O. Buu, B. Camarota, and K. C. Schwab, Science **304**, 74 (2004).
[8] D. H. Niblett, and J. Wilks, Adv. Phys. **9**, 1 (1960).
[9] K. P. Menard, *Dynamic Mechanical Analysis: A Practical Introduction*, 2nd ed. (CRC Press, Boca Raton, Florida, 2008).
[10] H. B. Yu, X. Shen, Z. Wang, L. Gu, W. H. Wang, and H. Y. Bai, Phys. Rev. Lett. **108**, 015504 (2012).
[11] T. S. Kê, Phys. Rev. **71**, 533 (1947).
[12] P. G. Debenedetti, and F. H. Stillinger, Nature **410**, 259 (2001).
[13] C. A. Angell, K. L. Ngai, G. B. McKenna, P. F. McMillan, and S. W Martin, J. Appl. Phys. **88**, 3113 (2000).
[14] A. L. Greer, Science **267**, 1947 (1995).
[15] W. H. Wang, C. Dong, and C. H. Shek, Mater. Sci. Eng. R **44**, 45 (2004).
[16] H. B. Yu, W. H. Wang and H. Y. Bai, Appl. Phys. Lett. **96**, 081902 (2010).
[17] Y. Q. Cheng, and E. Ma, Prog. Mater. Sci. **56**, 379 (2011).
[18] H. B. Yu, W. H. Wang, and K. Samwer, Mater. Today **16**, 183 (2013).
[19] H. B. Yu, W. H. Wang, H. Y. Bai, and K. Samwer, Natl. Sci. Rev. **1**, 429 (2014).
[20] M. Schwabe, D. Bedorf, and K. Samwer, Euro. Phys. J. E **34**, 1 (2011).
[21] C. Haon, D. Camel, B. Drevet, and J. M. Pelletier, Metal. Mater. Trans. A **39**, 1791 (2008).
[22] T. Ichitsubo, E. Matsubara, T. Yamamoto, H. S. Chen, N. Nishiyama, J. Saida, and K. Anazawa, Phys. Rev. Lett. **95**, 245501 (2005).
[23] M. Barmatz, and H. S. Chen, Phys. Rev. B **9**, 4073 (1974).
[24] B. S. Berry, W. C. Pritchet, and C. C. Tsuei, Phys. Rev. Lett. **41**, 410 (1978).
[25] N. Morito, and T. Egami, Acta Metall. **32**, 603 (1984).
[26] V. A. Khonik, and L. V. Spivak, Acta Mater. **44**, 367 (1996).
[27] V. A. Khonik, J. Phys. IV (France) **06**, C8–591 (1996).
[28] Y. Cohen, S. Karmakar, I. Procaccia, and K. Samwer, Europhys. Lett. **100**, 36003 (2012).
[29] M. I. Mendelev, M. J. Kramer, R. T. Ott, D. J. Sordelet, D. Yagodin, and P. Popel, Philos. Mag. **89**, 967 (2009).
[30] W. L. Johnson, and K. Samwer, Phys. Rev. Lett. **95**, 195501 (2005).
[31] W. L. Johnson, M. D. Demetriou, J. S. Harmon, M. L. Lind, and K. Samwer, MRS Bull. **32**, 644 (2007).
[32] R. Yamamoto, and A. Onuki, Phys. Rev. E **58**, 3515 (1998).
[33] W. K. Kegel, and A. van Blaaderen, Science **287**, 290 (2000).
[34] N. V. Priezjev, Phys. Rev. E **87**, 052302 (2013).
[35] J. P. Sethna, K. A. Dahmen and C. R. Myers, Nature **410**, 242 (2001).
[36] J. O. Krisponeit, S. Pitikaris, K. E. Avila, S. Kuchemann, A. Kruger, and K. Samwer, Nat. Commun. **5**, 3616 (2014).
[37] D. L. Turotte, Rep. Prog. Phys. **62**, 1377 (1999).
[38] U. R. Pedersen, T. B. Schrøder, J. C. Dyre, and P. Harrowell, Phys. Rev. Lett. **104**, 105701 (2010).
[39] H. L. Peng, M. Z. Li, and W. H. Wang, Phys. Rev. Lett. **106**, 135503 (2011).
[40] Y. Q. Cheng, H. W. Sheng, and E. Ma, Phys. Rev. B **78**, 014207 (2008).
[41] H. Reichert, Nature **408**, 839 (2000).
[42] Q. Wang, C. T. Liu, Y. Yang, Y. Dong, and J. Lu, Phys. Rev. Lett. **106**, 215505 (2011).
[43] H. B. Yu, K. Samwer, W. H. Wang, and H. Y. Bai, Nat. Commun. **4**, 2204 (2013).